8-15-2004

Franck-Condon Effects In Collision-Induced Electronic Energy Transfer: I2(E;v=1,2)+He,Ar

Pooja P. Chandra , '03

Thomas Alex Stephenson
Swarthmore College, tstephe1@swarthmore.edu

Franck-Condon effects in collision-induced electronic energy transfer: I 2 (E;v=1,2)+ He , Ar

Pooja P. Chandra and Thomas A. Stephenson

Citation: The Journal of Chemical Physics **121**, 2985 (2004); doi: 10.1063/1.1773158
View online: http://dx.doi.org/10.1063/1.1773158
View Table of Contents: http://scitation.aip.org/content/aip/journal/jcp/121/7?ver=pdfcov
Published by the AIP Publishing

Franck-Condon effects in collision-induced electronic energy transfer: $I_2(E;v=1,2)+He,\ Ar$

Pooja P. Chandra[a] and Thomas A. Stephenson[b]
Department of Chemistry and Biochemistry, Swarthmore College, 500 College Avenue, Swarthmore, Pennsylvania 19081

(Received 3 March 2004; accepted 24 May 2004)

Collisions of I_2 in the E electronic state with rare gas atoms result in electronic energy transfer to the D, β, and D' ion-pair electronic states. Rate constants for each of these channels have been measured when I_2 is initially prepared in the $J=55$, $v=1$ and 2 levels in the E state. The rate constants and effective hard sphere collision cross sections confirm the trends observed when $v=0$ in the E state is initially prepared: He collisions favor population of the D state, while Ar collisions favor population of the β state. Final state vibrational level distributions are determined by spectral simulation and are found to be qualitatively consistent with the trends in the Franck-Condon factors. The experimental distributions are also compared to the recent quantum scattering calculations of Tscherbul and Buchachenko. © *2004 American Institute of Physics.*
[DOI: 10.1063/1.1773158]

I. INTRODUCTION

Over the past decade, the availability of double resonance excitation schemes has enabled a number of detailed studies of the inelastic collision dynamics of I_2 in the ion-pair electronic states.[1–10] These states, which are common to all of the diatomic halogens, correlate with ionic halogen atoms, and are characterized by large dissociation energies (for I_2, $D_e \approx 31\,000\ cm^{-1}$) and equilibrium bond lengths that are substantially longer than those of the lower-lying valence states.[11] From the standpoint of inelastic dynamics, they represent a model system with which to examine collision-induced electronic energy transfer dynamics, particularly when coupled with the ability to prepare single rovibrational levels using optical-optical double resonance excitation.

Figure 1 displays the lowest energy portion of the so-called first tier of I_2 ion-pair states—those states which correlate to the lowest energy ionic asymptote, $I^+(^3P_2)+I^-(^1S_0)$. Note the presence of six electronic states with T_e values that lie within 1500 cm^{-1} of one another. This compact manifold of states allows one to examine in great detail the propensity rules for the changes in vibrational excitation that accompany electronic energy transfer. Previous investigations of this phenomenon have been largely limited to light diatomic species such as CN, N_2^+, and CO, in which a relatively sparse set of vibrational levels, accidental resonances, and fluctuating vibrational overlap integrals have made it difficult to develop theoretical models that hold predictive value for dissimilar species.[12] In contrast, the halogen ion-pair states, when coupled with the flexibility of double resonance excitation, present an opportunity to fine tune initial conditions and the range of final state energy gaps and/or vibrational overlaps.

In an early application of double resonance excitation to this problem, Ubachs *et al.* examined the $D \rightarrow X$ emission spectrum that results when I_2 is prepared in a single rotational level in $v=8$ of the E ion-pair state.[1] The presence of emission from the D state is attributed to $E \rightarrow D$ electronic energy transfer induced by $I_2(E)+I_2(X)$ collisions. Teule *et al.* have expanded on this work by considering a range of initial E state vibrational levels and a number of collision partners.[2] For example, they find that when $I_2(X)$ is the collision partner, energy gap effects dominate the distribution of vibrational populations in D state when certain E state levels are initially prepared, while Franck-Condon effects are more important when other vibrational levels are initially populated. When Ar is the collision partner, near-resonant energy transfer is preferred, regardless of the magnitude of the vibrational overlap integrals.[2]

Akopyan *et al.* have carried out extensive studies of the $E \rightarrow D$ electronic energy transfer that occurs following excitation of the E state, $v=8-58$, with a variety of atomic and molecular collision partners.[4–8] The cross section for electronic energy transfer is found to be quite large ($>10^3$ Å^2) when $I_2(X)$ is the collision partner, and the D state vibrational distributions are dominated by near-resonant energy transfer.[4,6] With rare gas (He,Ar) collision partners, the distributions of D state vibrational energy are found to be somewhat broader, with Ar collisions populating a wider range of vibrational levels than He.[5,7] The distributions are centered at or near the near-resonant D state vibrational level. Little correlation is observed with the E-D Franck-Condon factors. In the case of collisions with CF_4, evidence is found for vibrational excitation of the collision partner, leading to significant population in D state vibrational levels that differ from near resonance with the initially prepared E state level.[5,7]

In work previously reported from this laboratory, Fecko *et al.* examined the electronic energy transfer that occurs when E, $v=0$, $J=55$ collides with $I_2(X)$, He, and Ar.[9,10] In

[a]Current address: Weill Cornell Medical College, New York, NY 10021.
[b]Author to whom correspondence should be addressed.

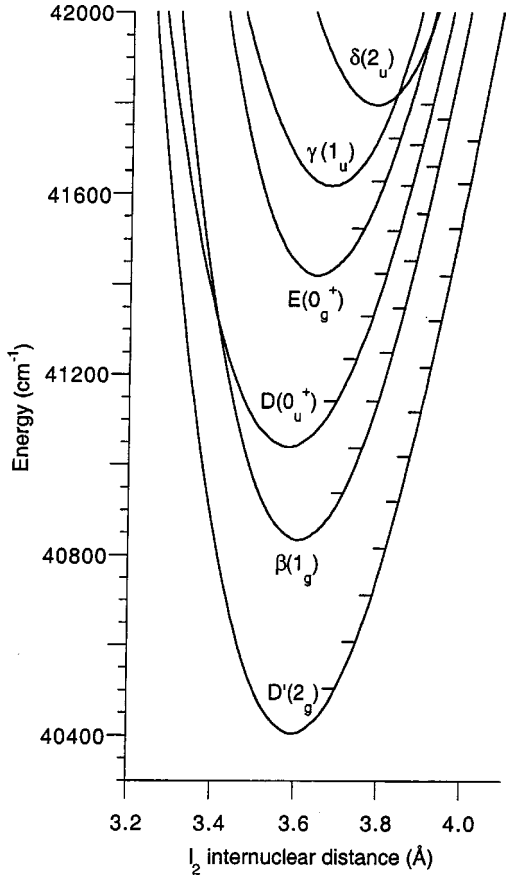

FIG. 1. Potential energy curves for the lowest tier ion-pair states in I_2. The horizontal tick marks indicate the energies of the vibrational energy levels ($J=55$).

the case of $I_2(X)$ collisions, population of the D state is found with a vibrational distribution that is intermediate to that expected from strict application of either Franck-Condon or energy gap considerations.[9] With rare gas collision partners, collision-induced electronic energy transfer results in population of the D, D', and β electronic states.[10] The vibrational distributions suggest that while both Franck-Condon and energy gap effects are important in $E \rightarrow D$ electronic energy transfer, vibrational overlap considerations become more important when the final electronic state is D' or β. The overall cross section for electronic energy transfer for $Ar+I_2$ collsions is found to be approximately three times that for $He+I_2$ collisions.[10]

In parallel with these experimental developments, Tscherbul and Buchachenko have initiated a theoretical examination of the $E \rightarrow D$, $E \rightarrow \beta$, and $E \rightarrow D'$ electronic energy transfer induced by collisions with He and Ar.[13–16] In this work, Ar/I_2 and He/I_2 potential energy surfaces were obtained utilizing the first-order intermolecular diatomics-in-molecule perturbation theory approach.[13] The dynamics are treated at varying levels of approximation. Initial semiclassical calculations focused on the $E \rightarrow D$ electronic energy transfer that occurs in $Ar+I_2$ collisions.[14] More recently, these calculations have been extended to include a more sophisticated quantum treatment of the dynamics of $Ar+I_2$ and $He+I_2$ collisions, along with the $E \rightarrow D'$ and $E \rightarrow \beta$ relaxation channels.[15,16]

With the goals of exploring the generality of our previous experimental investigations, and comparing with the emerging theoretical analysis of electronic energy transfer in I_2, we have extended our experiments to include excitation of I_2 to the E ion-pair state, $v=1$ and 2. After a brief summary of our experimental methodology (Sec. II), we will focus on the presentation of our experimental data, with a special emphasis on comparison with the theoretical calculations of Tscherbul and Buchachenko, which have been extended to the same level of vibrational excitation in the E state.

II. EXPERIMENT

The experimental strategy used in these investigations has been described in previous publications from this laboratory.[9,10] Briefly, we prepare I_2 in a single rotational level ($J=55$) of either the $v=1$ or 2 vibrational levels of the E ion-pair electronic state using two-color double resonance excitation. For preparation of $v=1$, the initial $B \leftarrow X$ excitation occurs via the (21,0), $R(55)$ transition; the required 557.18 nm radiation is provided by a Nd^{3+}-YAG pumped dye laser (Continuum Lasers YG580-30/TDL-50) operating with Rhodamine 575 laser dye (Exciton). After a delay of 5–10 ns, the second photon excites a fraction of the B state population using the $E \leftarrow B(1,21)$, $P(56)$ transition at 426.34 nm. This photon is provided by a N_2-pumped dye laser (Laser Photonics UV24/DL-14P) operating with Coumarin 440 laser dye (Exciton). For excitation of $v=2$ in the E state, we utilize the (23,0), $R(55)$, $B \leftarrow X$ transition at 551.90 nm and the (2,23), $P(56)$, $E \leftarrow B$ transition at 427.66 nm. Both lasers have a pulse width of 10 ns. The timing between the excitation lasers is controlled by a digital delay generator (Berkeley Nucleonics 555) and is variable over a wide range of delays. The emission features reported here occur only when the N_2 laser system fires coincident with or later than the YAG laser system; no emission is observed when one of the laser beams is blocked from reaching the sample chamber. The YAG-pumped dye laser operates with a spectral bandwidth of ≈ 0.15 cm^{-1}; the bandwidth of the N_2-pumped dye laser is ≈ 0.25 cm^{-1}.

Double resonance excitation of I_2 results in intense $E \rightarrow B$ emission between 415 and 435 nm, as well as a number of weaker features, depending on the sample pressure conditions. I_2 emission is collected by an f/1.2 fused silica optical system, and is focused onto the entrance slit of a 0.5 m focal length scanning monochromator (Instruments SA 500M). The monochromator is equipped with a 2400 groove/mm grating, providing a dispersion of 0.8 nm/mm. Typical slit widths are 100–200 μm. Wavelength resolved emission exiting the monochromator is detected by replacing the exit slit with a CCD camera (Princeton Instruments LN/CCD-2500PB). Each of the 2500 pixel columns on the CCD chip is 12 μm wide, providing a total spectral coverage of 24 nm and a data point spacing of 0.0096 nm.

I_2 vapor, at a pressure of 40 mTorr, and a variable pressure of either He or Ar were held in a glass and fused silica

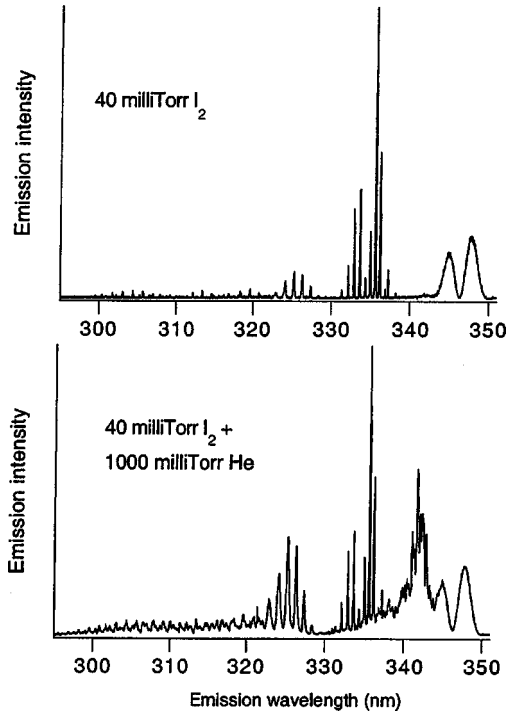

FIG. 2. Emission spectra from I_2, following excitation of $v=1$, $J=55$ in the E electronic state. Upper frame: the sample is I_2 only. Lower frame: the sample is I_2+1000 mTorr of He.

cell, equipped with Brewster's angle laser inlet and exit windows. The cell was filled on a glass vacuum line pumped by a diffusion pump/mechanical pump combination to a base pressure of $\approx 2\times 10^{-5}$ Torr. All pressures were measured with a capacitance manometer (MKS Baratron 127 series) with a precision of ± 1 mTorr. I_2 (Aldrich, 99.999%), He (MG, 99.9999%), and Ar (MG, 99.9995%) were used without additional purification.

Analysis of our emission spectra and the electronic energy transfer pathways required a number of Franck-Condon factors, which we calculated using the LEVEL program from Rydberg-Klein-Rees (RKR) potential energy curves.[17] We determined the RKR curves from the spectroscopic data provided in the literature for the E,[18] D',[19] and A (Ref. 20) states. We utilized directly the literature RKR curves for the D,[21] β,[22] A',[23] and X (Ref. 24) states.

III. RESULTS AND DISCUSSION

In Fig. 2, portions of the wavelength resolved emission spectra that result when I_2 is prepared in the E electronic state, $v=1$, $J=55$ are displayed. The spectrum in the upper panel is obtained when the sample consists of I_2 only; the spectrum in the lower panel results from a mixture of I_2 and He. Similar spectra (not shown) are obtained when Ar is the added rare gas, and when $v=2$ is the initially excited E state level. In addition to the $E\rightarrow B''$ (343–350 nm) and $E\rightarrow A$ (331–338 nm) emission systems observed in the absence of collision partner, we observe features in the 295–329 nm wavelength range, assigned to $D\rightarrow X$ emission. The emission with peak intensity near 340 nm is due to the overlapping $D'\rightarrow A'$ and $\beta\rightarrow A$ electronic systems. [Weak $D\rightarrow X$ emission is also observed in the absence of a rare gas collision partner. This emission is the result of $E\rightarrow D$ electronic transfer induced by $I_2(E)+I_2(X)$ collisions, as discussed in our previous work.[9]) In all cases, the integrated intensity of the D and D'/β state emission is found to be linearly dependent on the rare gas pressure. Using a kinetic analysis described in our previous publications,[9,10] we determine the rate constants for electronic energy transfer and the effective hard sphere collision cross sections. These results are displayed in Table I where we have incorporated the results for $v_E=0$ from our earlier work for comparison.[10] Inspection of the rate constants reveals that the trends identified in our previous work

TABLE I. Rate constants and effective cross sections for electronic energy transfer.

Initial E state vibrational level	Collision partner	Final electronic state	Rate constant (10^{-17} m^3 s^{-1} molecule^{-1})	Effective hard sphere collision cross section (Å^2)	Total cross section (all final states; Å^2)
0[a]	He	D	3.8±0.5	3.0±0.4	
		D'	1.1±0.2	0.9±0.2	4.9±0.5
		β	1.2±0.2	1.0±0.2	
	Ar	D	2.0±0.4	4.7±0.9	
		D'	1.0±0.2	2.4±0.4	14±1.4
		β	3.0±0.5	7.0±1.0	
1	He	D	5.2±1.3	4.1±1.0	
		D'	3.6±0.5	2.8±0.4	9.7±1.2
		β	3.5±0.5	2.8±0.4	
	Ar	D	2.5±1.3	5.9±3.0	
		D'	2.1±0.8	4.8±1.8	19±4.7
		β	3.6±1.3	8.4±3.1	
2	He	D	6.4±0.8	5.1±0.6	
		D'	4.7±1.8	3.7±1.5	13±2.2
		β	4.8±1.9	3.8±1.5	
	Ar	D	3.2±2.1	7.5±4.9	
		D'	3.8±1.4	8.9±3.4	29±7.8
		β	5.7±2.1	13 ±5.0	

[a]$v=0$ data taken from Ref. 10.

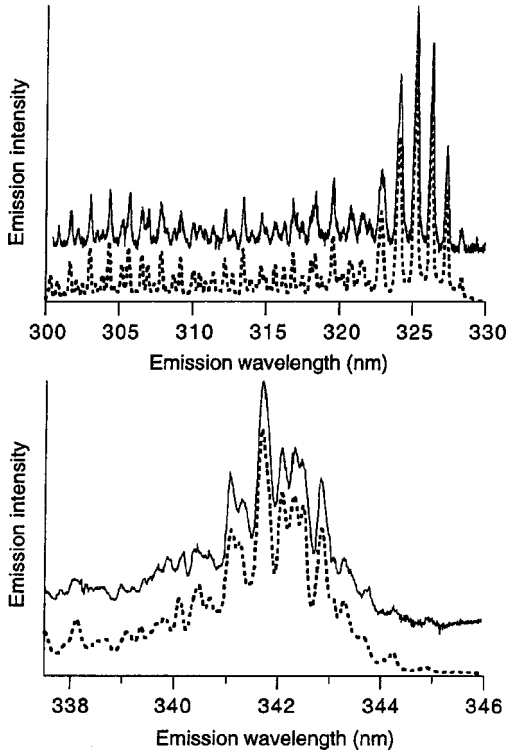

FIG. 3. I_2 emission induced by collisions with He. Experimental data: solid lines. Simulation: dashed lines. The experimental spectrum is offset for clarity. Upper frame: $D \rightarrow X$ emission; He pressure is 250 mTorr. Lower frame: $D' \rightarrow A'$ and $\beta \rightarrow A$ emission; He pressure is 1000 mTorr.

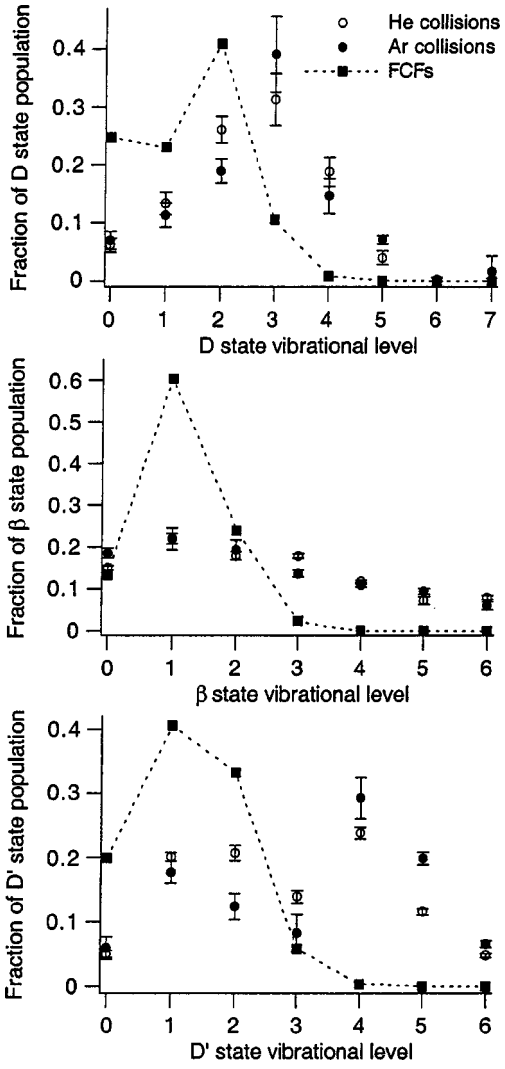

FIG. 4. Vibrational population distributions resulting from collision-induced electronic energy transfer following excitation of $v=1$, $J=55$ in the E electronic state. He collisions: open circles, Ar collisions: filled circles. Franck-Condon factors linking E, $v=1$ with the final vibronic state: filled squares/dashed line. Upper frame: D electronic state. Middle frame: β electronic state. Lower frame: D' electronic state.

appear to be followed with increasing values of v_E. Specifically, collisions with He favor population of the D electronic state, while Ar collisions favor population of the β electronic state, though the degree of selectivity appears to diminish as v_E increases. In addition, we note that the total cross section for electronic energy transfer increases with v_E for both He and Ar and that, for all v_E, the total cross section is larger for Ar/I_2 collisions than for He/I_2. The increase with v_E in the electronic energy transfer cross section is generally in accord with the work of Akopyan *et al.*, who found that the cross section for $E \rightarrow D$ energy transfer increases with v_E over the range $v_E=8$ to ≈ 30, at which point it levels off at a value of ≈ 60 Å^2.[7] The cross section for He collisions is generally lower than that for Ar collisions, though the trend is not as consistent as that displayed in Table I.

In Fig. 3, the $D \rightarrow X$ and $D' \rightarrow A'/\beta \rightarrow A$ portions of the spectrum that result from excitation of I_2 to the E electronic state, $v=1$, $J=55$ in the presence of He are seen, along with our best fits to these regions. The variable parameters in our fits are the populations of the $v=0-7$ levels in the D state, and $v=0-6$ in the β and D' states. In each case, all of the major features in the experimental spectra are reproduced in our fits with this limited set of vibrational populations. Based on the signal-to-noise level in our spectra and the expected Franck-Condon distribution of emission intensities, we estimate the higher vibrational levels contribute less than 10% to the vibrational populations.

In Fig. 4, we present the D, D', and β state vibrational distributions that result when $I_2(E,v=1)$ collides with He and Ar. In Fig. 5, the same information is presented, except that I_2 is prepared in the $v=2$ level of the E state. Note that in every case, the distributions that result from He and Ar collisions are largely the same. We noted previously that qualitatively, the vibrational distributions that result from $I_2(E,v=0)+$He, Ar collisions were in accord with the Franck-Condon factors (FCFs) that represent the vibrational overlap between the initially excited and final vibrational levels.[10] Also plotted in Figs. 4 and 5 are the relevant $E-D$, $E-\beta$, and $E-D'$ FCFs. Populations in the D state roughly follow the trend in FCFs, in the sense that the most highly populated level shifts to higher v when the FCFs follow that trend. For $v_E=1$ and 2, and for both collision partners, the experimental D state distributions peak at one unit of v higher than the maximum FCF.

The distributions of population in the β and D' states were found to be peaked at the Franck-Condon maximum when E, $v=0$ is the initial state. Figures 4 and 5 demonstrate that when $v=1$ and 2 are prepared, the β state distributions

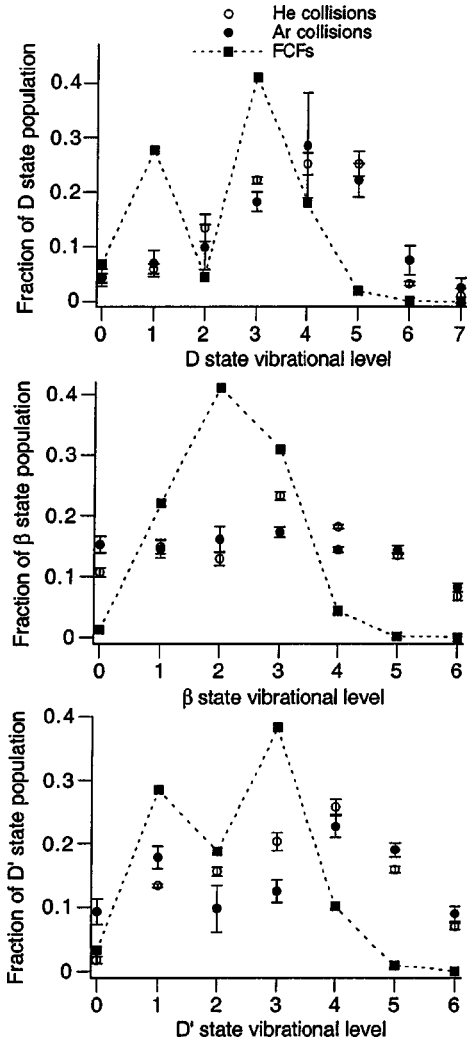

FIG. 5. Vibrational population distributions resulting from collision-induced electronic energy transfer following excitation of $v=2$, $J=55$ in the E electronic state. He collisions: open circles. Ar collisions: filled circles. Franck-Condon factors linking E, $v=2$ with the final vibronic state: filled squares/dashed line. Upper frame: D electronic state. Middle frame: β electronic state. Lower frame: D' electronic state.

are relatively flat, though the most populated level shifts to higher v, following the trend in the FCFs. For the β state, the overall distribution is broader and less structured for the higher values of v_E, consistent with the patterns in the FCFs. The broadening of the distribution with v_E is also observed in the case of the D' state populations, though when $v_E=1$, the D' state experimental distributions takes on a bimodal appearance that is not reproduced in the FCFs. When $v_E=2$, the experimental distribution also exhibits a bimodal distribution, which is reproduced in the FCFs in this case. The plots shown in Figs. 4 and 5 demonstrate that, in general, the vibrational populations in the D' state adhere to the Franck-Condon factors to a greater degree than in the case of the D state, with the β state populations representing an intermediate case. To quantify this trend, in Table II we have tabulated the average amount of vibronic energy transferred ($\langle \Delta E_{\mathrm{vib}} \rangle$) for the three final electronic states and for $v_E=0$, 1, and 2 for collisions with He. (Since the distributions that result from Ar collisions are nearly quantitatively the same as for He collisions, we have omitted the values of $\langle \Delta E_{\mathrm{vib}} \rangle$ for Ar collisions for clarity.) In addition, Table II displays the values of $\langle \Delta E_{\mathrm{vib}} \rangle$ that result from the Franck-Condon distribution along with the ratio of the experimental average energy transferred to the Franck-Condon average. In each case the experimental figures are smaller than those based on the Franck-Condon model, though the disparity is largest for the D state and smallest for the D' state.

TABLE II. Average vibronic energy transferred in $I_2(E)+\mathrm{He}$ collisions.

Final electronic state	Initial E state vibrational level	Experimental $\langle \Delta E_{\mathrm{vib}} \rangle$ (cm^{-1})	Franck-Condon model $\langle \Delta E_{\mathrm{vib}} \rangle$ (cm^{-1})	Experimental/ Franck-Condon
D	0	249	350	0.71
	1	243	353	0.69
	2	256	357	0.72
β	0	438	571	0.77
	1	436	568	0.77
	2	488	564	0.86
D'	0	938	985	0.95
	1	828	991	0.84
	2	881	988	0.89

These differences among the D, β, and D' state distributions can be understood by considering the balance between the magnitude of the FCFs and the vibronic energy gaps involved in the energy transfer transitions. For $v_E=0$, 1, and 2, the near resonant D state vibrational levels are characterized by FCFs that are less than 4×10^{-4}, providing a significant vibrational overlap impediment to population of levels with small energy gaps. Just the same, the availability of D state vibrational levels with significant (but not optimal) FCFs, combined with modest vibronic energy gaps, appears to direct population into levels that balance these two considerations. For example, when $v_E=2$, the D state vibrational distribution peaks at $v_D=4$. While this energy transfer channel has a FCF that is 44% of the maximum (at $v_D=3$) in the FCFs, it also corresponds to a 31% smaller vibronic energy gap.

The balance between energy gap and Franck-Condon effects shifts to place greater reliance on the latter when the D' and β states are populated. The larger values of ΔT_{e} for $E\rightarrow\beta$ and $E\rightarrow D'$ electronic energy transfer dictate that near resonant transfer involves larger values of Δv and correspondingly very small FCFs. For example, when $v_E=1$, near-resonant energy transfer would populate $v=7$ in the β state and $v=11$ in the D' state. All of the final state levels with non-negligible vibrational overlap involve large vibronic energy gaps. For example, when $v_E=2$, all of the D' state levels with $E-D'$ FCFs that are greater than 1×10^{-2} have vibronic energy gaps that exceed 800 cm^{-1}. In these cases, the dynamics direct population into channels with large energy gaps and large FCFs, in preference to small energy gaps and very small FCFs.

As noted in the Introduction, Tscherbul and Buchachenko have initiated a series of calculations which explore the $E\rightarrow D$, $E\rightarrow\beta$, and $E\rightarrow D'$ collision-induced electronic energy transfer. A preliminary report on these efforts, focusing on the $E\rightarrow D$ transfer that accompanies $\mathrm{Ar}+\mathrm{I}_2$ (E, v

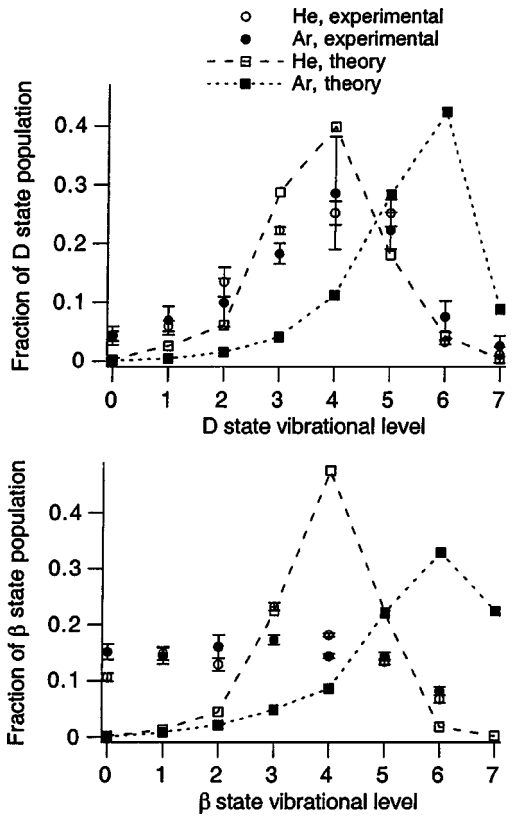

FIG. 6. Comparison of theory and experiment for electronic energy transfer from E, $v=2$, $J=55$. Upper frame: D electronic state vibrational distribution. Lower frame: β electronic state vibrational distribution.

$=0$, 8, and 16) collisions, has been published.[14] For this semiclassical treatment of the dynamics, an intermolecular diatomics-in-molecules potential energy surface is used to represent the Ar–I_2 interaction.[13] This potential energy surface has a minimum ($D_e=217\,cm^{-1}$) in the perpendicular, T-shaped geometry and a saddle-point in the linear geometry. These calculations produce a rate constant for $E\rightarrow D$ energy transfer that is in reasonable agreement with the experimental data, though the D state vibrational distribution is more narrow and is peaked at a level that is much closer to near-resonant transfer than observed experimentally.[14]

More recently, the same potential energy surface (and an analogous construction for the He-I_2 interaction) have been used in close coupling calculations in which all six first tier electronic states are incorporated. In addition, initial excitation of both $v_E=0$ and 2 are considered.[15,16] Selected results of these calculations are shown in Fig. 6, along with the relevant experimental data. Focusing first on the D state vibrational distributions (upper panel), we observe that the calculations are in excellent agreement with the experimental distribution when He is the collision partner. Agreement with the distribution that results from Ar collisions is less satisfactory; the theoretical distribution peaks at vibrational levels higher than observed experimentally. Larger discrepancies are observed when the $E\rightarrow\beta$ energy transfer is considered. Here the agreement with the He results is only qualitative, and the distribution resulting from Ar collisions shows strong deviations from the experimental data, similar to those observed for the D state population distribution. This pattern is repeated for the calculated D' state distributions (not shown).

The analysis of Tscherbul and Buchachenko demonstrates that the $E\rightarrow D$ electronic energy transfer occurs by a different mechanism than $E\rightarrow\beta$ and $E\rightarrow D'$ transfer.[15,16] Specifically, $E\rightarrow D$ energy transfer is dominated by the impulsive interaction of the rare gas atom with the repulsive wall of the potential energy surface. Energy transfer to the β and D' states are a secondary effect, induced by state mixing upon recoil into the vicinity of the attractive portions of the potential. This interpretation is in agreement with the experimental observation that the rate constants for $E\rightarrow\beta$ and $E\rightarrow D'$ channels are diminished when He is the collision partner (as compared to Ar collisions). The weaker attractive He–I_2 potential will contribute a smaller degree of final states interaction in the recoiling partners.

Overall, the comparison of theory and experiment points to possible deficiencies in the potential energy surfaces, particularly for the Ar-I_2 interaction. The lack of agreement between the calculated vibrational distributions and the experimental measurements may be due to an underestimation of the attractive interactions in the ion-pair states. Indeed the Ar-I_2 interaction used in the current model is weaker than those for the X and B electronic states,[25] while the opposite trend is observed in matrix isolation and cluster studies.[26,27] Further, it is now generally accepted that the Ar-I_2 interaction has a substantial potential minimum corresponding to the linear Ar-I-I configuration,[28–30] a feature that is missing in the current potential. Given the ability of Ar to polarize the I_2 molecule, the omission of this enhanced attraction along the I_2 internuclear axis may be a significant weakness. These attractive effects are larger for Ar-I_2 than He–I_2 and the superior agreement of the He collision-induced vibrational distributions with the experimental values suggests that refinements are required in the model of the rare gas-I_2 attractive interactions, particularly for the heavier rare gas atoms. The experimental data presented in this work should provide the basis for quantitative adjustments to the depth, range, and angular anisotropy of this potential interaction in the ion-pair states. We anticipate that the on-going exchange between theory and experiment will illuminate and reinforce critical aspects of our emerging understanding of collision-induced electronic energy transfer.

ACKNOWLEDGMENTS

This work has been supported by grants from the Camille and Henry Dreyfus Foundation and the Swarthmore College Faculty Research Fund. We are grateful to Professor A. Buchachenko and Professor A. Pravilov for sharing results prior to publication, and for many fruitful exchanges of views. We also acknowledge the valuable experimental assistance of J. Lillvis and S. Johnson.

[1] W. Ubachs, I. Aben, J. B. Milan, G. S. Somsen, A. G. Stuiver, and W. Hogervorst, Chem. Phys. **174**, 285 (1993).
[2] R. Teule, S. Stolte, and W. Ubachs, Laser Chem. **18**, 111 (1999).
[3] D. Inard, D. Cerny, M. Nota, R. Bacis, S. Churassy, and V. Skorokhodov, Chem. Phys. **243**, 305 (1999).
[4] M. E. Akopyan, N. K. Bibinov, D. B. Kokh, A. M. Pravilov, and M. B. Stepanov, Chem. Phys. **242**, 263 (1999).

[5] M. E. Akopyan, N. K. Bibinov, D. B. Kokh, A. M. Pravilov, O. L. Sharova, and M. B. Stepanov, Chem. Phys. **263**, 459 (2001).
[6] N. K. Bibinov, O. L. Malinina, A. M. Pravilov, M. B. Stepanov, and A. A. Zakharova, Chem. Phys. **277**, 179 (2002).
[7] M. E. Akopyan, A. M. Pravilov, M. B. Stepanov, and A. A. Zakharova, Chem. Phys. **287**, 399 (2003).
[8] M. E. Akopyan, I. Yu. Chinkova, T. V. Fedorova, S. A. Poretsky, and A. M. Pravilov, Chem. Phys. **302**, 61 (2004).
[9] C. J. Fecko, M. A. Freedman, and T. A. Stephenson, J. Chem. Phys. **115**, 4132 (2001).
[10] C. J. Fecko, M. A. Freedman, and T. A. Stephenson, J. Chem. Phys. **116**, 1361 (2002).
[11] J. C. D. Brand and A. R. Hoy, Appl. Spectrosc. Rev. **23**, 285 (1987).
[12] P. J. Dagdigian, Annu. Rev. Phys. Chem. **48**, 95 (1997).
[13] T. V. Tscherbul, A. V. Zaitsevskii, A. A. Buchachenko, and N. F. Stepanov, Russ. J. Phys. Chem. **77**, 511 (2003).
[14] T. V. Tscherbul and A. A. Buchachenko, Chem. Phys. Lett. **370**, 563 (2003).
[15] T. V. Tscherbul and A. A. Buchachenko, J. Phys. B **37**, 1605 (2004).
[16] A. A. Buchachenko (private communication).
[17] R. J. LeRoy, University of Waterloo Chemical Physics Research Report, No. CP-230R3, 1986.
[18] J. C. D. Brand, A. R. Hoy, A. K. Kalker, and A. B. Yamashita, J. Mol. Spectrosc. **95**, 350 (1982).
[19] X. Zheng, S. Fei, M. C. Heaven, and J. Tellinghuisen, J. Chem. Phys. **96**, 4877 (1992).
[20] D. R. T. Appadoo, R. J. Le Roy, P. F. Bernath *et al.*, J. Chem. Phys. **104**, 903 (1996).
[21] T. Ishiwata and I. Tanaka, Laser Chem. **7**, 79 (1987).
[22] J. P. Perot, M. Broyer, J. Chevalyre, and B. Femelat, J. Mol. Spectrosc. **98**, 161 (1983).
[23] D. Cerny, R. Bacis, S. Churassy, D. Inard, M. Lamrini, and M. Nota, Chem. Phys. **216**, 207 (1997).
[24] F. Martin, R. Bacis, S. Churassy, and J. Vergès, J. Mol. Spectrosc. **116**, 71 (1986).
[25] A. Buchachenko, N. Halberstadt, B. Lepetit, and O. Roncero, Int. Rev. Phys. Chem. **22**, 153 (2003).
[26] M. Macler and M. C. Heaven, Chem. Phys. **151**, 219 (1991).
[27] S. Fei, X. Zheng, M. C. Heaven, and J. Tellinghuisen, J. Chem. Phys. **97**, 6057 (1992).
[28] C. F. Kunz, I. Burghardt, and B. A. Heß, J. Chem. Phys. **109**, 359 (1998).
[29] A. E. Stevens Miller, C.-C. Chuang, H. C. Fu, K. J. Higgins, and W. Klemperer, J. Chem. Phys. **111**, 7844 (1999).
[30] R. Prosmiti, P. Villarreal, and G. Delgado-Barrio, Chem. Phys. Lett. **359**, 473 (2002).